Inorganic Chemistry

ARTICLE

pubs.acs.org/IC

A Highly Selective Redox, Chromogenic, and Fluorescent Chemosensor for Hg^{2+} in Aqueous Solution Based on Ferrocene−Glycine Bioconjugates

Arunabha Thakur, Sinjinee Sardar, and Sundargopal Ghosh*

Department of Chemistry, Indian Institute of Technology Madras, Chennai 600 036, India

Supporting Information

ABSTRACT: The synthesis, electrochemical, optical, and metal-cation-sensing properties of ferrocene−glycine conjugates $C_{30}H_{38}O_8N_8Fe$ (**2**) and $C_{20}H_{24}O_4N_4Fe$ (**3**) have been documented. Both compounds **2** and **3** behave as very selective redox ($\Delta E_{1/2}$ = 217 mV for **2** and $\Delta E_{1/2}$ = 160 mV for **3**), chromogenic, and fluorescent chemosensors for Hg^{2+} cations in an aqueous environment. The considerable changes in their absorption spectra are accompanied by the appearance of a new low-energy peak at 630 nm (**2**, ε = 1600 M^{-1} cm^{-1}; **3**, ε = 822 M^{-1} cm^{-1}). This is also accompanied by a strong color change from yellow to purple, which allows a prospective for the "naked eye" detection of Hg^{2+} cations. These chemosensors present immense brightness and fluorescence enhancement (chelation-enhanced fluorescence = 91 for **2** and 42 for **3**) following Hg^{2+} coordination within the limit of detection for Hg^{2+} at 7.5 parts per billion.

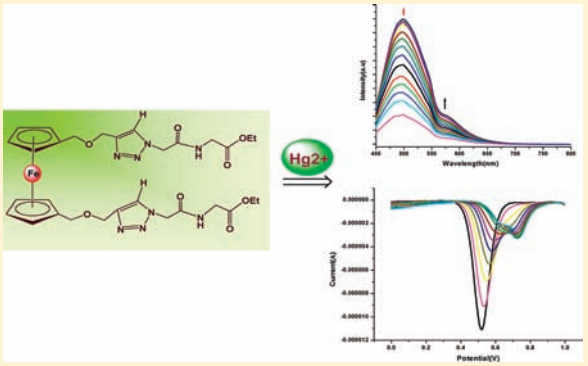

INTRODUCTION

The mercuric ion is considered to be one of the most toxic elements among heavy- and soft-metal cations, and the sensitive detection of Hg^{2+} ion is currently a task of key importance for environmental and biological concerns.[1−4] However, the design and advancement of new and practical chemosensors that offer a promising advance for mercuric ion detection is still a great challenge in supramolecular chemistry.[5−10] To develop sensitive Hg^{2+} sensors, various receptors consisting of a mercuric ion recognition unit and a probe exhibiting physical responses upon coordination of Hg^{2+} have been reported.[11] Among them, ferrocene derivatives are often applied to redox sensors because of their unique electrochemical properties.[12] In addition, the robustness of ferrocene under aerobic conditions and the ease of functionalization have made ferrocene a favorite molecule for conjugation to biomolecules.[13]

Although several colorimetric,[14] redox-active,[15] and fluorescence-based chemosensors[16] have been extensively investigated for the determination of Hg^{2+} ions, certain constraints are encountered; for example, (i) mercuric ion can cause fluorescence quenching of the fluorophores via the spin−orbit coupling effect;[17] thus, most of the probes were designed based on fluorescence quenching;[18−23] (ii) many of the sensors contain hydrophobic fluorophores that demand the addition of organic cosolvents to increase their solubility in aqueous media.[24] Therefore, searching for Hg^{2+} probes based on fluorescence enhancement, which is more sensitive than fluorescence quenching, is still an active field in analytical chemistry.[25−28] Here in this article, we demonstrate the synthesis, characterization, optical, and electrochemical properties of two new ferrocene−glycine bioconjugates, **2** and **3**, that selectively detect Hg^{2+} ions in aqueous solution. Furthermore, a sensitive fluorescent probe for Hg^{2+} has been recognized with a very low limit of detection.

EXPERIMENTAL SECTION

Materials and Methods. Perchlorate salts of Li^+, Na^+, K^+, Ca^{2+}, Mg^{2+}, Cr^{2+}, Mn^{2+}, Fe^{2+}, Co^{2+}, Cu^{2+}, Zn^{2+}, Cd^{2+}, Ni^{2+}, Pb^{2+}, and Hg^{2+}, propargyl bromide, butyllithium, and tetramethylethylenediamine purchased from Aldrich were used directly without further purification. Ferrocene, sodium ascorbate, glycine ethyl ester hydrochloride, sodium azide, and acetonitrile were purchased and used without further purification. *N*,*N*-Dimethylformamide was purchased from Aldrich and freshly distilled prior to use. Chromatography was carried out on 3 cm of silica gel in a column of 2.5 cm diameter. Column chromatography was carried out using 60−120 mesh silica gel. All of the solvents were dried by conventional methods and distilled under a N_2 atmosphere before use. Ethyl 2-(2-azidoacetamido)acetate[29] and compounds $[Fc(CH_2OCH_2C{\equiv}CH)_n]$ (**1a**, n = 2; **1b**, n = 1; Fc = ferrocene) were synthesized as per literature procedures.[30] Cyclic voltammetry (CV) and differential pulse voltammetry (DPV) were performed with a conventional three-electrode configuration consisting of glassy carbon as a working electrode, platinum as an auxiliary electrode, and Ag/Ag^+ as a reference electrode. The experiments were carried out with a 10^{-3} M solution of the sample

Received: March 21, 2011
Published: June 27, 2011

Scheme 1. Synthesis of Mono- and Di-ferrocene−Glycine Conjugates 2 and 3

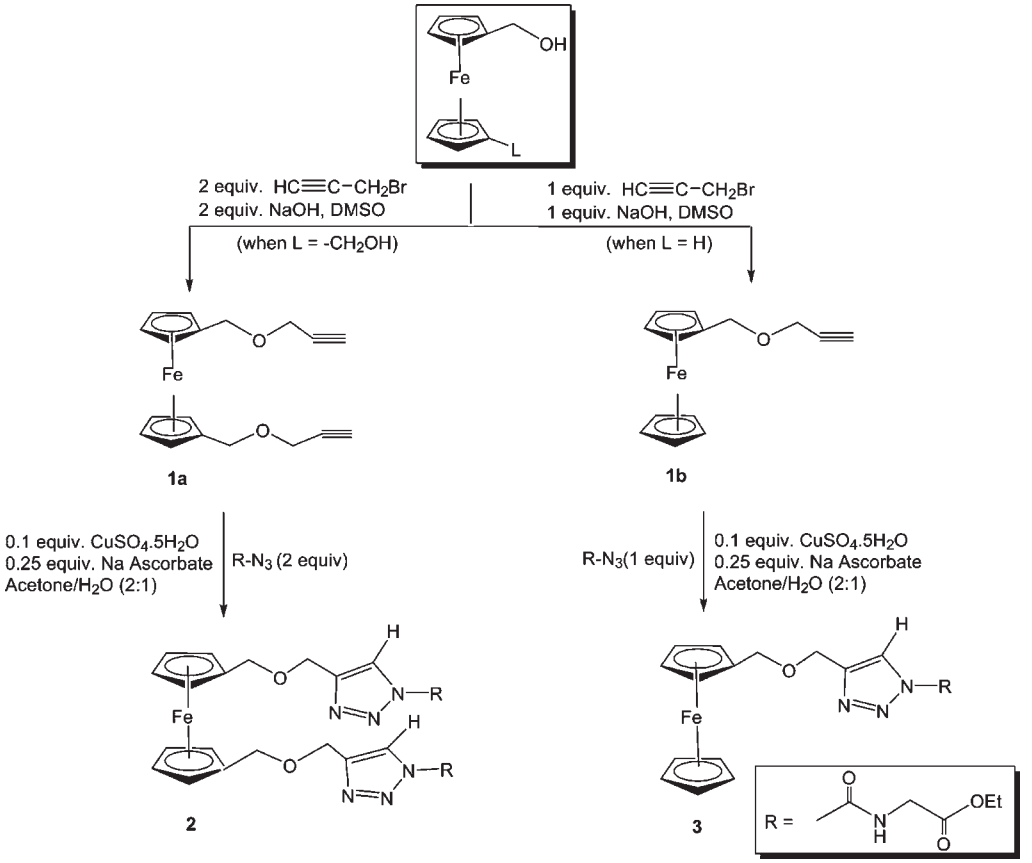

in CH_3CN or CH_3CN/H_2O (2:8) containing 0.1 M $(n\text{-}C_4H_9)_4NClO_4$ as a supporting electrolyte. Deoxygenation of the solutions was achieved by bubbling nitrogen for at least 10 min, and the working electrode was cleaned after each run. The cyclic voltammograms were recorded at a scan rate of 0.1 V s^{-1}. The UV−vis spectra were carried out in CH_3CN or CH_3CN/H_2O (2:8) solutions at $c = 1 \times 10^{-4}$ M, whereas the fluorescence spectra were carried out in water at $c \approx 10^{-8}$ M, as stated in the corresponding figure captions.

Instrumentation. The ^1H and ^{13}C NMR spectra were recorded on Bruker 400 and 500 MHz FT-NMR spectrometers, using tetramethylsilane as the internal reference. Electrospray ionization mass spectrometry (ESI-MS) measurements were carried out on a Qtof Micro YA263 HRMS instrument. The absorption spectra were recorded with a Jasco V-650 UV−vis spectrophotometer at 298 K. The CV and DPV measurements were performed on a CH potentiostat model 668. The fluorescence was recorded with a Jasco FP-6300 spectrofluorimeter.

Caution! *Metal perchlorate salts are potentially explosive in certain conditions. All due precautions should be taken while handling perchlorate salts!*

Synthesis of Ferrocene−Glycine Conjugates 2 and 3. To a well-stirred solution of **1a** (0.5 g, 1.55 mmol) and azide (0.576 g, 3.1 mmol) in 15 mL of acetone/H_2O (2:1) was added an aqueous solution of $CuSO_4 \cdot 5H_2O$ (0.077 g, 0.31 mmol). To the mixture was added a freshly prepared sodium ascorbate solution (0.122 g, 0.62 mmol), and the resulting solution was stirred at room temperature for 12 h. A total of 30 mL of ethyl acetate was added to the reaction mixture, and the organic layer was washed several times with water and finally with brine (15 mL) and dried over anhydrous sodium sulfate. The solvent was removed under reduced pressure, and the crude product was purified by silica gel column chromatography. Elution with EtOAc/hexane (8:2, v/v) yielded yellow **2** (0.95 g, 88%).

Compound **3** was prepared in good yield following the procedure adopted for **2** from alkyne **1b** (0.5 g, 1.96 mmol), azide (0.364 g, 1.96 mmol), aqueous $CuSO_4 \cdot 5H_2O$ (0.097 g, 0. 392 mmol), and sodium ascorbate (0.149 g, 0.776 mmol). The crude product was purified by silica gel column chromatography and elution with EtOAc/hexane (7:2, v/v) to yield pure yellow **3** (0.73 g, 85%).

2. ^1H NMR ($CDCl_3$, 400 MHz): δ 7.70 (s, 2H), 7.10 (s, 2H), 5.07 (s, 4H), 4.56 (s, 4H), 4.32 (q, 4H), 4.25 (s, 4H), 4.03−4.09 (t, 8H), 3.95 (d, 4H), 1.23 (t, 3H). ^{13}C NMR ($CDCl_3$, 100 MHz): δ 169.38, 165.83, 145.54, 124.55, 69.92, 68.95, 68.32, 62.95, 61.70, 52.60, 41.44, 14.16. ESI-MS (relative intensity): m/z 717 (M^+ + 23, 100).

3. ^1H NMR ($CDCl_3$, 400 MHz): δ 7.67 (s, 1H), 6.94 (s, 1H), 5.06 (s, 2H), 4.58 (s, 2H), 4.32 (q, 2H), 4.26 (s, 2H), 4.15−4.16 (t, 9H), 3.95 (d, 2H), 1.24 (t, 3H). ^{13}C NMR ($CDCl_3$, 100 MHz): δ 169.24, 165.59, 145.88, 124.38, 69.95, 68.96, 68.83, 62.97, 61.7, 52.64, 41.41, 14.12. ESI-MS (relative intensity): m/z 441 (M^+ + 1), 463 (M^+ + 23).

RESULTS AND DISCUSSION

Synthesis. Precursors **1a** and **1b** were obtained following literature procedures.[30] They undergo the "click reaction" with ethyl 2-(2-azidoacetamido)acetate to produce compounds **2** and **3** in 88% and 85% yields, respectively (Scheme 1). Compounds **2** and **3** have been characterized by ESI-MS, the usual spectroscopic and analytical techniques, IR and ^1H and ^{13}C NMR spectroscopy. Both compounds **2** and **3** are moderately stable and could be stored at 10 °C for months. The complexation

dx.doi.org/10.1021/ic200573m |*Inorg. Chem.* 2011, 50, 7066–7073

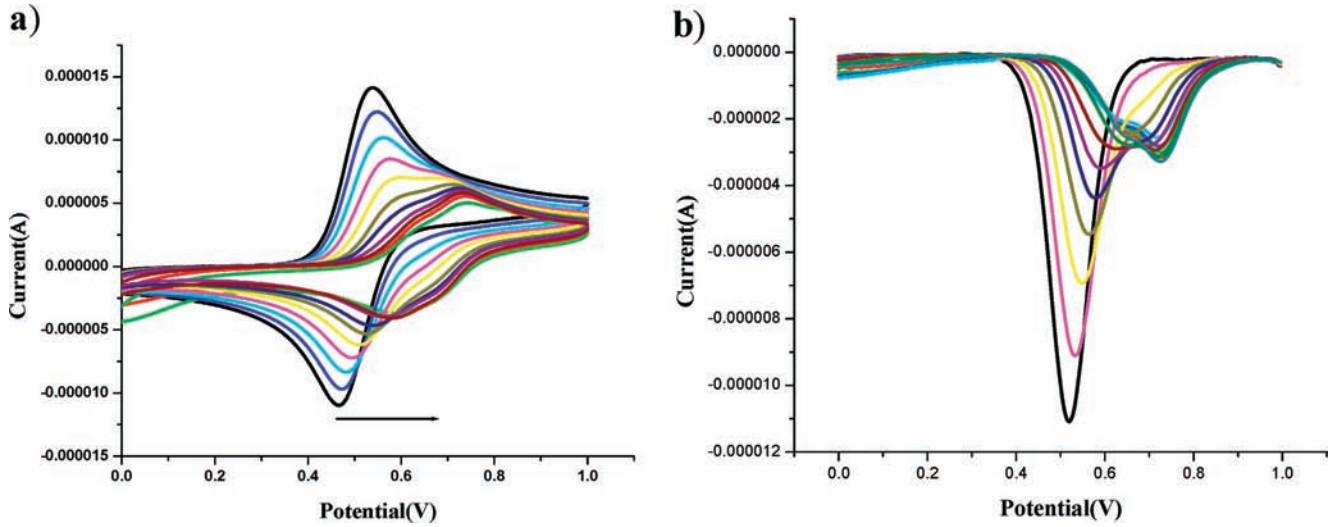

Figure 1. Evolution of CV (a) and DPV (b) of **2** (10^{-3} M) in CH_3CN using $[(n\text{-}Bu)_4N]ClO_4$ as the supporting electrolyte when 0−1 equiv of $Hg(ClO_4)_2$ is added.

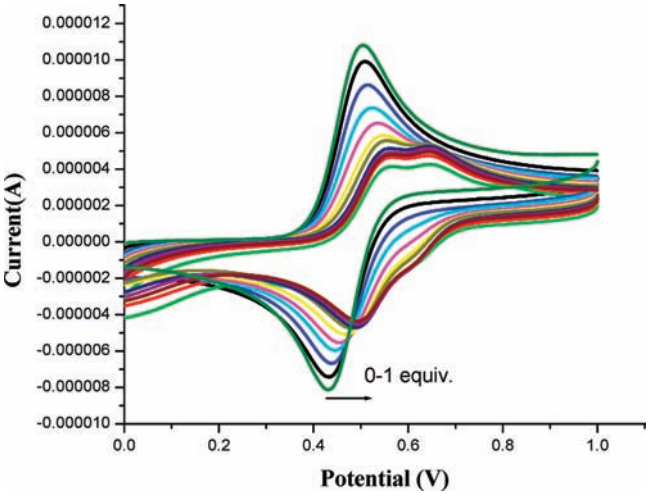

Figure 2. Evolution of the CV of **3** (10^{-3} M) in CH_3CN using $[(n\text{-}Bu)_4]ClO_4$ as the supporting electrolyte upon the addition of increasing amounts of Hg^{2+} metal cation up to 1 equiv. The arrow indicates the movement of the wave during the experiments.

properties of the receptors **2** and **3** have been investigated by electrochemistry, UV−vis, and fluorescence spectroscopic measurements.

Electrochemical Studies. Chemical sensors bearing ferrocene nuclei as part of the sensing unit have been broadly studied. Earlier, the complexation of ferrocene with a variety of binding ligands has been studied by CV, and it showed a positive shift of the Fe^{II}/Fe^{III} redox couple as a result of metal−ligand complexation.[31] The metal-recognition properties of receptors **2** and **3** were evaluated by CV and DPV analysis. The reversibility and relative oxidation potential of the redox process were determined by CV and DPV in CH_3CN solutions containing 0.1 M $[(n\text{-}Bu)_4N]ClO_4$ as the supporting electrolyte. Both **2** and **3** display a reversible one-electron oxidation process at $E_{1/2}$ = 0.495 and 0.466 V, respectively, due to the ferrocene/ferrocenium redox couple. No perturbation of the cyclic and differential pulse voltammograms of **2** and **3** was observed in the presence of several metal cations such as Li^+, Na^+, K^+, Ca^{2+}, Mg^{2+}, Cr^{2+}, Zn^{2+}, Ni^{2+}, Fe^{2+}, Co^{2+}, Cd^{2+}, and Pb^{2+} as their appropriate salts, even in large excess. However, as shown in Figures 1 and 2, the original peak gradually decreased upon the stepwise addition of Hg^{2+} ions, while a new peak, associated with the formation of a complexed species, appeared at 0.712 V ($\Delta E_{1/2}$ = 217 mV) and 0.627 V ($\Delta E_{1/2}$ = 160 mV) for **2** and **3**, respectively.

In addition, linear sweep voltammetry (LSV) studies, shown in Figure 3, carried out upon the addition of Cu^{2+} to a CH_3CN solution of receptor **2** showed a significant shift of the voltammetric wave toward the cathodic current, indicating that this metal cation promotes oxidation of the free receptor with its concomitant reduction to Cu^+. This is in agreement with CV (Supporting Information, Figure S2). By contrast, the same experiment carried out upon the addition of Hg^{2+} cations revealed a shift of the LSV toward a more positive potential (Figure 3), which is in agreement with the complexation process previously observed by CV (Figure 1). Remarkably, the redox response toward Hg^{2+} is also preserved in the presence of an aqueous environment [CH_3CN/H_2O (2:8, v/v)]. The DPV measurements show no shift following complexation with Hg^{2+} in a aqueous CH_3CN solution.

UV−Vis Absorption Studies. The UV−vis binding interaction studies of receptors **2** and **3** in CH_3CN (1×10^{-4} M) against cations of environmental relevance, such as of Li^+, Na^+, K^+, Ca^{2+}, Mg^{2+}, Cr^{2+}, Zn^{2+}, Fe^{2+}, Ni^{2+}, Co^{2+}, Cd^{2+}, and Pb^{2+} as perchlorate salts, show selective response to Hg^{2+} and Cu^{2+}. The changes in the UV−vis absorbance spectra of receptors **2** and **3** in CH_3CN due to the stepwise addition of Hg^{2+} ion are shown in the Figures 4 and 5. Upon the addition of 1 equiv of Hg^{2+} to **2**, the high-energy (HE) absorption band at λ = 312 nm (ε = 7200 M^{-1} cm^{-1}) was red-shifted to 324 nm ($\Delta\delta$ = 12 nm; ε = 15 400 M^{-1} cm^{-1}). The HE band at λ = 311 nm was red-shifted to 321 nm ($\Delta\delta$ = 10 nm; ε = 6890 M^{-1} cm^{-1}) in the case of **3**. In addition, as shown in Figures 4 and 5, a new and weak lower-energy (LE) absorption band appeared at λ = 630 nm for both **2** (ε = 1600 M^{-1} cm^{-1}) and **3** (ε = 822 M^{-1} cm^{-1}). These facts are responsible for the change of color from yellow to purple, which is visible to the naked eye. Binding assays using the method of continuous variations (Job's plot) strongly suggest 1:1 (cation/receptor) complex formation with Hg^{2+} ion both for compounds **2** (Figure 4b)

dx.doi.org/10.1021/ic200573m |*Inorg. Chem.* 2011, 50, 7066–7073

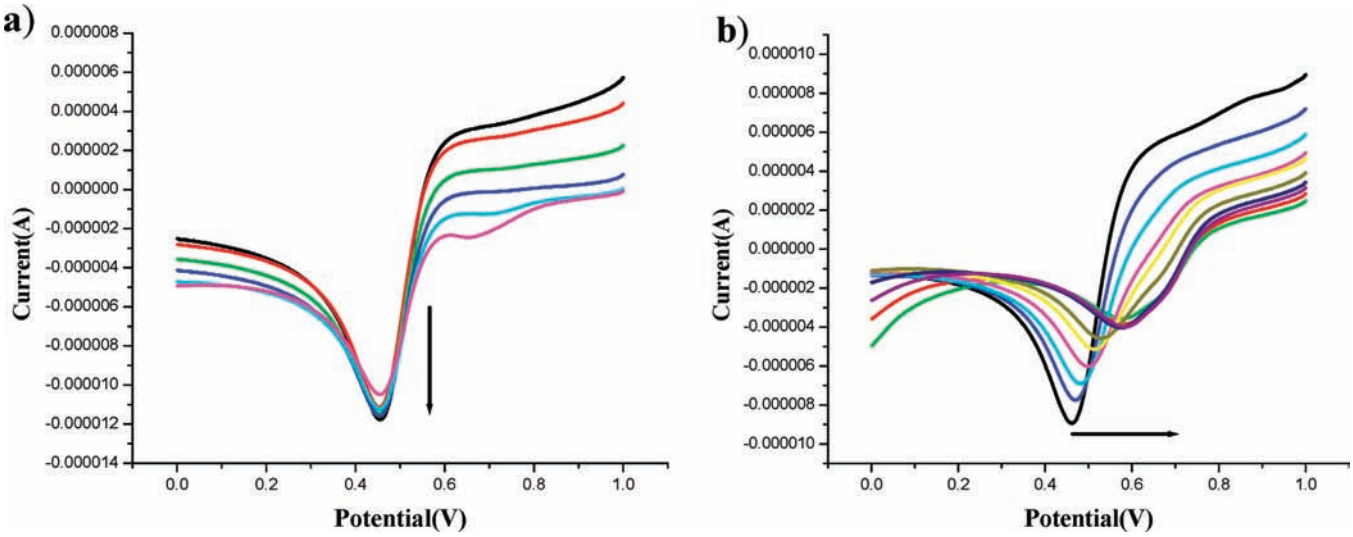

Figure 3. Evolution of LSV of **2** (10^{-3} M) in CH_3CN during the addition of Cu^{2+} (a) and Hg^{2+} (b) with $[(n\text{-}Bu)_4N]ClO_4$ as the supporting electrolyte scanned at 0.1 V s^{-1}.

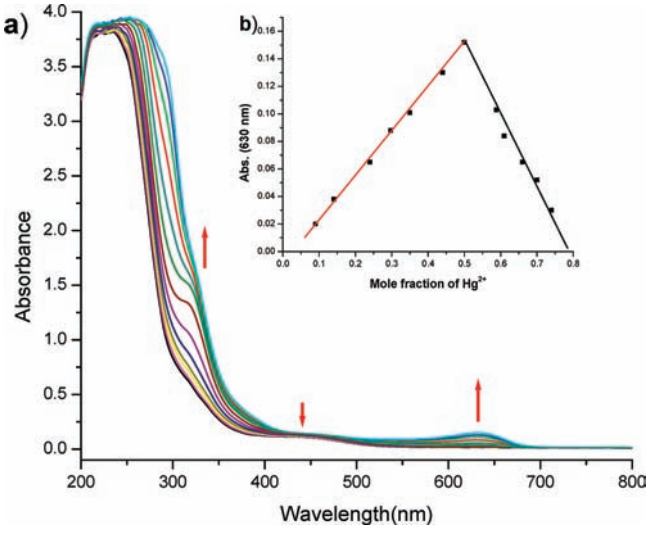

Figure 4. (a) Changes in the absoption spectra of **2** (10^{-4} M) in CH_3CN upon the addition of increasing amounts of Hg^{2+} up to 1 equiv. (b) Job's plot for **2** and Hg^{2+}, indicating the formation of 1:1 complexes. The total $[\mathbf{2}] + [Hg^{2+}] = 1 \times 10^{-4}$ M.

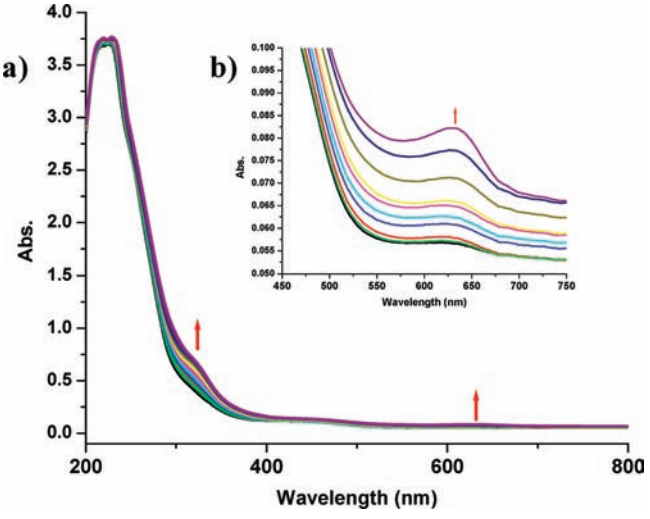

Figure 5. (a) Changes in the absoption spectra of **3** (10^{-4} M) in CH_3CN upon the addition of increasing amounts of Hg^{2+} up to 1 equiv. (b) Expanded form of part a.

and **3** (Supporting Information, Figure S5). The stoichiometries of the complexes have also been confirmed by ESI-MS, where peaks at m/z 895 for the $[\mathbf{2}\cdot Hg^{2+}]$ complex and at m/z 639 for the $[\mathbf{3}\cdot Hg^{2+}]$ complex are observed (Supporting Information, Figures S6 and S7).

Likewise, the addition of increasing amounts of Cu^{2+} ions to a solution of **2** showed the progressive appearance of one HE band at 294 nm (ε = 9900 M^{-1} cm^{-1}) and one LE band at 637 nm with the concomitant decrease of the initial HE band intensities at 252 nm (ε = 17 400 M^{-1} cm^{-1}). Two well-defined isosbestic points at ca. 400 and 250 nm were found, indicating that only one spectrally distinct complex was present. The new LE band at 637 nm is accountable for the change of color from yellow to bluish green that can be used for the "naked eye" detection of Cu^{2+} ions. The UV−vis spectral change, shown in Figure 6, suggests that the ferrocene moiety is oxidized upon complexation with Cu^{2+} ions, and the change of color to green is characteristic of the formation of the ferrocenium ion.[32] The binding assays using the method of continuous variations (Job's plot) suggests a 1:1 (cation/receptor) complex formation for compound **2** (Figure 6b).

The UV−vis absorbance change of receptor **3** in CH_3CN (1×10^{-4} M) due to the addition of Cu^{2+} ions was also evaluated (Supporting Information, Figure S10). Previous studies showed that the binding event of the charged species with a ferrocene-based receptor can perturb the LE band, generally leading to a bathochromic (red) shift upon complexation.[33] The band at 434 nm of free receptor **3** was bathochromically shifted to 625 nm after the addition of 0.5 equiv of Cu^{2+} ions. However, in contrast to **2**, the further addition of Cu^{2+} leads to quenching of the band, and it completely disappeared at 1 equiv (Supporting Information, Figure S11). The addition of Cu^{2+} ion above 1 equiv did not

dx.doi.org/10.1021/ic200573m |*Inorg. Chem.* 2011, 50, 7066–7073

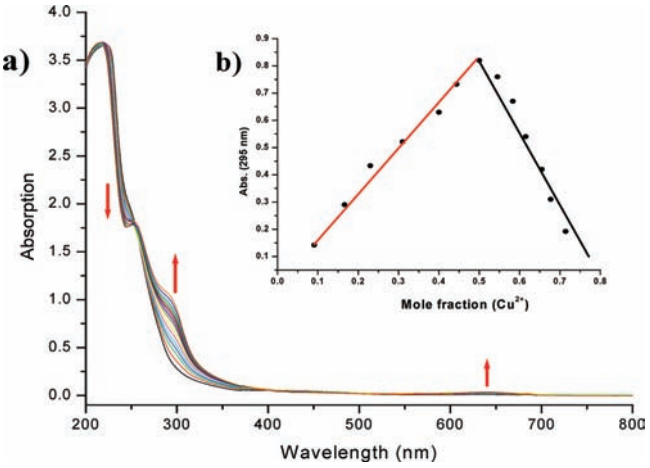

Figure 6. (a) Changes in the absoption spectra of **2** (10^{-4} M) in CH_3CN upon the addition of increasing amounta of Cu^{2+} metal cation up to 1 equiv. (b) Job's plot for **2** and Cu^{2+}, indicating the formation of 1:1 complexes.

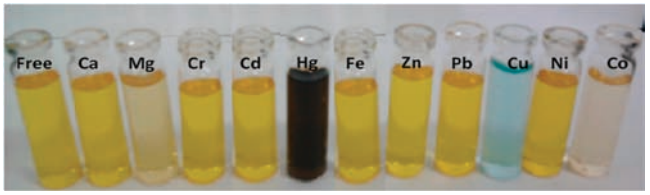

Figure 7. Visual features observed in CH_3CN solution of **2** (10^{-3} M) after the addition of 10 equiv of different metal cations tested.

show any considerable change. The dependence of the absorption at 625 nm on the Cu^{2+} ion concentration suggests that two types of complexes, first 2:1 followed by 1:1 host−guest complexes, are formed. These results are also supported by the ESI-MS spectra (Supporting Information, Figures S6 and S7).

Visual Detection of Hg^{2+} and Cu^{2+}. When an excess of different metal ions (Li^+, Na^+, K^+, Ca^{2+}, Mg^{2+}, Cr^{2+}, Zn^{2+}, Ni^{2+}, Co^{2+}, Fe^{2+}, Cd^{2+}, Hg^{2+}, and Pb^{2+}) is separately added to a solution of **2** and **3** in CH_3CN (10^{-3} M), no significant color change is observed, except for Hg^{2+} and Cu^{2+}. As shown in Figure 7, Hg^{2+} shows a drastic color change from yellow to purple, whereas Cu^{2+} shows a color change from yellow to bluish green. Although Co^{2+} shows a slight color change, no significant changes are observed in the UV−vis, CV, and fluorescence spectroscopy. The sensing potential of **3** toward Hg^{2+} and Cu^{2+} in solution is very similar to **2**.

Fluorescent Detection of Hg^{2+} in Water. The widely used sensing method of fluorescent recognition has been utilized for the quantification of various molecules.[34] Compared to other approaches, fluorescent sensing shows excellent sensitivity, rapid response, and the capability of doing recognition in a nondestructive manner.[35] Thus, the extent to which the fluorescence intensities of receptors **2** and **3** were affected in the presence of the selected cations was tested by fluorescence spectroscopy. Both the receptors **2** and **3** exhibit a very weak fluorescence in CH_3CN solution ($c = 2.5 \times 10^{-8}$ M for **2** and 10^{-7} M for **3**) when excited at $\lambda_{exc} = 434$ nm. The emission spectra of both receptors shows bands at 499 nm with quantum yields (Φ)[36] of 6.6×10^{-4} and 6.1×10^{-4}, respectively. However, in the presence of Hg^{2+} ion, the

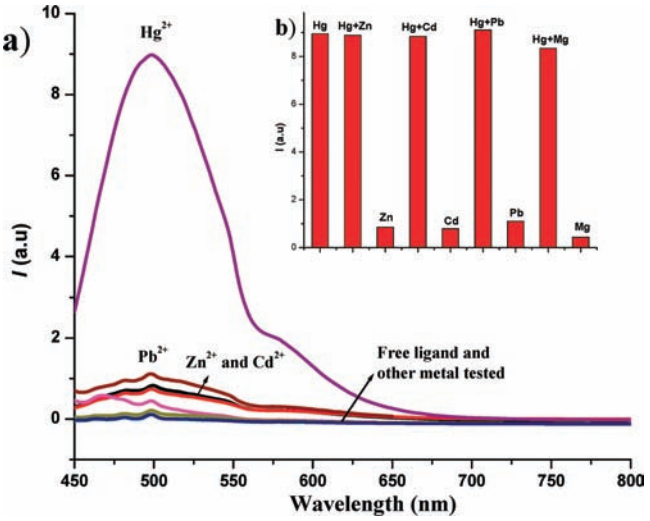

Figure 8. (a) Changes in the fluorescence spectra of **2** (2.5×10^{-8} M) in water upon the addition of the several cations tested. (b) Fluorescence emission intensity of **2** upon the addition of 0.5 equiv of Hg^{2+} in the presence of 0.5 equiv of interference metal ions in water.

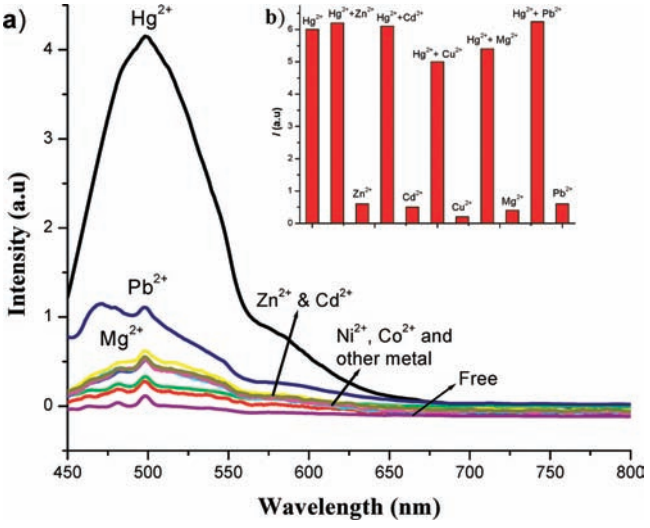

Figure 9. Changes in the fluorescence spectra of **3** (10^{-7} M) in water upon the addition of the several cations tested. (b) Fluorescence emission intensity of **3** upon the addition of 0.5 equiv of Hg^{2+} in the presence of 0.5 equiv of interference metal ions in water.

emission band yielded an important enhancement of the emission band (CHEF[37] = 91 for **2** and 42 for **3**). The quantum yield ($\Phi = 2.1 \times 10^{-2}$) resulted in a 32-fold increase compared to that of the free receptor **2** and a 15-fold increase compared to that of **3** ($\Phi = 9.7 \times 10^{-3}$) (Figures 8 and 9). The fluorescent behavior of receptors **2** and **3** in the presence of Cu^{2+}, Zn^{2+}, Cd^{2+}, and Pb^{2+} was also tested, and their emission spectra did not undergo any considerable changes.

To address the sensitivity of **2** toward Hg^{2+} sensing, we have carried out fluorescence titration of **2** (2.5×10^{-8} M) in water with Hg^{2+} (1×10^{-4} M). There is no such detectable change in the fluorescence spectra up to the analyte concentration of 0.2 equiv. An appreciable enhancement of the quantum yield by a factor of 4 is observed in the presence of 0.3 equiv of Hg^{2+},

dx.doi.org/10.1021/ic200573m |Inorg. Chem. 2011, 50, 7066–7073

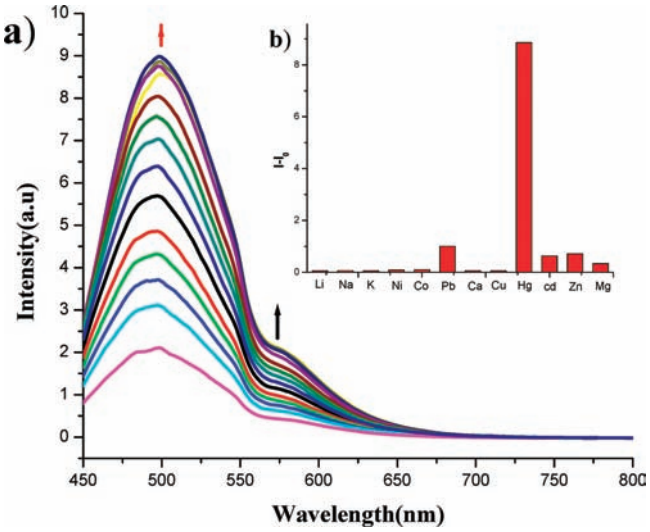

Figure 10. (a) Changes in the fluorescence spectra of receptor **2** (2.5×10^{-8} M) in water upon titration with Hg^{2+} (1×10^{-4} M). (b) Emission intensity of receptor **2** in water, with respect to a free ligand, after the addition of 1 equiv of several cations.

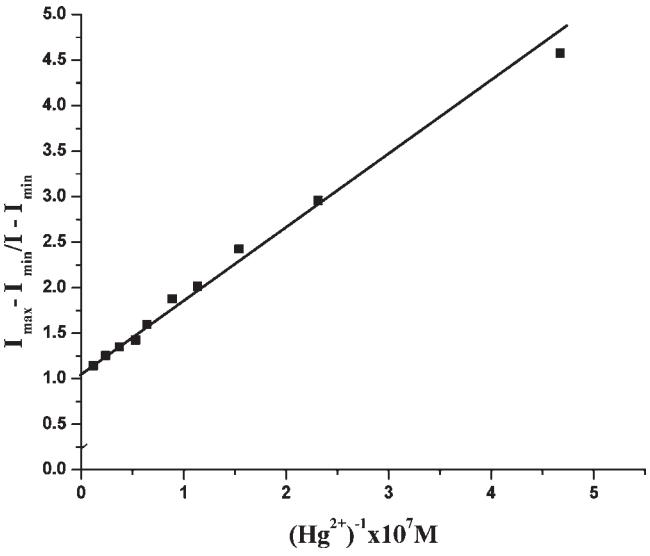

Figure 11. Benesi–Hildebrand plot of receptor **2** binding with Hg^{2+} ion (0–1 equiv) associated with fluorescence change.

whereas a maximum fluorescence enhancement was observed in the presence of 1 equiv of Hg^{2+} (Figure 10). This experiment shows that the low detectable limit of Hg^{2+} in a water medium with **2** is 7.5×10^{-9} M (7.5 ppb) in our experimental conditions. The binding constant value of Hg^{2+} with **2** has been determined from the emission intensity data following the modified Benesi–Hildebrand equation[38] $1/\Delta I = 1/\Delta I_{max} + (1/K[C])(1/\Delta I_{max})$ ($\Delta I = I - I_{min}$ and $\Delta I_{max} = I_{max} - I_{min}$, where I, I_{min}, and I_{max} are the emission intensities of **2** considered in an intermediate Hg^{2+} concentration, in the absence of Hg^{2+}, and at a concentration of complete interaction, respectively, K is the binding constant, and [C] is the Hg^{2+} concentration. From the plot of $(I_{max} - I_{min})/(I - I_{min})$ against $[C]^{-1}$, shown in Figure 11, the value of K (±15%) extracted from the slope is 6.75×10^6 M^{-1}.[39]

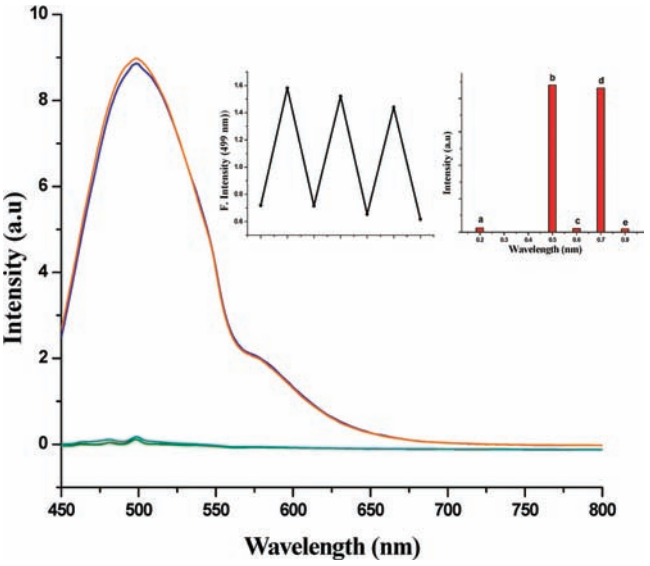

Figure 12. Reversibility of the interaction between **2** and Hg^{2+} by the introduction of I^- to the system. Column a represents the fluorescence intensity of **2** (1 μM); columns b and d represent the fluorescence intensities of **2** after the addition of 1 equiv of Hg^{2+}; columns c and e represent the fluorescence intensities of **2** after the introduction of I^- (5 equiv to Hg^{2+}). Inset: Stepwise complexation/decomplexation cycles carried out in CH_3CN with **2** and Hg^{2+}.

To evaluate further the importance of **2** and **3** as a Hg^{2+}-selective fluorescence probe, competition experiments were carried out. Thus, a solution of **2** and **3** (1×10^{-5} M) was treated separately with 0.5 equiv of Hg^{2+} in the presence of 0.5 equiv each of interference metal ions (Zn^{2+}, Cd^{2+}, Pb^{2+}, Mg^{2+}, and Cu^{2+}). From the resulting titrations, shown in Figures 8b and 9b, small or no obvious interference with the detection of Hg^{2+} could be observed. These results clearly demonstrate the selectivity for Hg^{2+} over the other metal ions.

Reversibility of the Interaction of 2 and Hg^{2+}. For a chemical sensor to be extensively employed in the detection of specific analytes, the reversibility is an important aspect. The interaction between **2** and Hg^{2+} was reversible, which was verified by the introduction of I^- into the system containing **2** (1 μM) and Hg^{2+} (2 equiv). The experiment, shown in Figure 12, showed that the introduction of I^- (5 equiv to Hg^{2+}) immediately quenched the fluorescence of **2**. When Hg^{2+} was added to the system again, the fluorescence of **2** was enhanced. This process could be repeated at least three times without a loss of sensitivity, which clearly demonstrates the high degree of reversibility of the complexation/decomplexation process.

To support the results obtained by electrochemical and spectroscopic experiments and to obtain additional information about the coordination mode of these metal cations by receptor **2**, we also performed a ^1H NMR spectroscopic analysis in CD_3CN solution. The most significant spectral changes (^1H NMR; Supporting Information, Figure S12) observed upon the addition of increasing amounts of Hg^{2+} ions to a solution of the free receptor **2** are the following: (i) Hg^{2+} metal ions caused broadening of the NH-(CH_2) and CH_2 protons in the ^1H NMR spectrum; (ii) the amine protons (δ = 7.33 ppm) move downfield ($\Delta\delta$ = 0.44 ppm); (iii) the hydrogen atom within the triazole ring showed a significant downfield shift by ca. 0.15 ppm; (iv) the observed downfield shifts for the cyclopentadienyl ring hydrogen atoms in ferrocene were

dx.doi.org/10.1021/ic200573m |*Inorg. Chem.* 2011, 50, 7066–7073

not prominent. From the magnitude of the observed ^{1}H chemical shifts, it can be concluded that complexation exerts a more powerful effect on both the triazole ring hydrogen atoms and amine protons than ferrocene ring hydrogen atoms.

CONCLUSION

In conclusion, we have described two simple triazole-based, easy-to-synthesize, and multisignaling chemosensors **2** and **3** that selectively bind with the Hg^{2+} cation. These chemosensors not only exhibit the capability of highly selective detection of Hg^{2+} cation through a fluorescent probe but also acquiesce to the facile colorimetric sensing of Hg^{2+} cation, thus allowing the potential for "naked-eye" detection over some other cations. Receptors **2** and **3**, the organometallic bioconjugates, show some advantages over other Hg^{2+} chemosensors, such as high selectivity for Hg^{2+} in neutral aqueous media through a fluorescence probe, short response time (<1 min), and low detection limit (7.5 ppb).

ASSOCIATED CONTENT

Supporting Information. ^{1}H, ^{13}C NMR, and ESI-MS data of **2** and **3**; electrochemical data for **2** and **3** upon titration with Cu^{2+} and different metal ions; UV−vis spectra upon titration with different metal ions; ESI-MS spectra of [**2**·Hg^{2+}], [**3**·Hg^{2+}], [**2**·Cu^{2+}], and [**3**·Cu^{2+}]; Benesi−Hildebrand plot of receptor **3** binding with a Hg^{2+} ion; evolution of ^{1}H NMR spectra of **2** in CD_3CN upon the addition of increasing amounts of Hg^{2+}, and Job's plot for the emission titration of **2** with Hg^{2+}. This material is available free of charge via the Internet at http://pubs.acs.org.

AUTHOR INFORMATION

Corresponding Author

*E-mail: sghosh@iitm.ac.in. Phone: (+91) 44 2257 4230. Fax: (+91) 44 2257 4202.

ACKNOWLEDGMENT

Generous support of the Indo-French Centre for the Promotion of Advanced Research (IFCPAR-CEFIPRA), New Delhi, India, under Grant 4405-1, is gratefully acknowledged. A.T. is grateful to the Council of Scientific and Industrial Research, India, for research fellowships and SAIF, IIT Madras, for NMR spectroscopy.

REFERENCES

(1) Martínez-Máñez, R.; Sancenón, F. *Chem. Rev.* **2003**, *103*, 4419.
(2) Callan, J. F.; de Silva, A. P.; Magri, D. C. *Tetrahedron* **2005**, *61*, 8551.
(3) de Silva, A. P.; Gunaratne, H. Q. N.; Gunnlaugsson, T.; Huxley, A. J. M.; McCoy, C. P.; Rademacher, J. T.; Rice, T. E. *Chem. Rev.* **1997**, *97*, 1515.
(4) (a) Benoit, J. M.; Fitzgerald, W. F.; Damman, A. W. *Environ. Res.* **1998**, *78*, 118. (b) Renzoni, A.; Zino, F.; Franchi, E. *Environ. Res.* **1998**, *77*, 68. (c) Malm, O. *Environ. Res.* **1998**, *77*, 73.(d) *Mercury Update: Impact on Fish Advisories*; EPA Fact Sheet EPA-823-F-01-011; EPA, Office of Water: Washington, DC, 2001.
(5) Caballero, A.; Martínez, R.; Lloveras, V.; Ratera, I.; Vidal-Gancedo, J.; Wurst, K.; Tárraga, A.; Molina, P.; Veciana, J. *J. Am. Chem. Soc.* **2005**, *127*, 15666.
(6) Díez-Gil, C.; Caballero, A.; Ratera, I.; Tárraga, A.; Molina, P.; Veciana, J. *Sensors* **2007**, *7*, 3481.
(7) Huang, J.; Xu, Y.; Qian, X. *J. Org. Chem.* **2009**, *74*, 2167.
(8) Lu, H.; Xiong, L.; Liu, H.; Yu, M.; Shen, Z.; Li, F.; You, X. *Org. Biomol. Chem.* **2009**, *7*, 2554.
(9) Gong, J.; Zhou, T.; Song, D.; Zhang, L.; Hu, X. *Anal. Chem.* **2010**, *82*, 567.
(10) Loe-Mie, F.; Marchand, G.; Berthier, J.; Sarrut, N.; Pucheault, M.; Blanchard-Desce, M.; Vinet, F.; Vaultier, M. *Angew. Chem., Int. Ed.* **2010**, *49*, 424.
(11) (a) Beer, P. D. *Chem. Soc. Rev.* **1989**, *18*, 409. (b) Czarnik, A. W. *Acc. Chem. Res.* **1994**, *27*, 302.
(12) Beer, P. D.; Gale, P. A.; Chen, G. Z. *Coord. Chem. Rev.* **1999**, *185*−*186*, 3.
(13) (a) Van Staveren, D. R.; Metzler-Nolte, N. *Chem. Rev.* **2004**, *104*, 5931–5985 and references therein. (b) Metzler-Nolte, N. *Angew. Chem., Int. Ed.* **2001**, *40*, 1040.
(14) (a) Brummer, O.; La Clair, J. J.; Janda, K. D. *Org. Lett.* **1999**, *1*, 415. (b) Choi, M. J.; Kim, M. Y.; Chang, S. K. *Chem. Commun.* **2001**, 1664. (c) Zhao, Y.; Zhong, Z. Q. *Org. Lett.* **2006**, *8*, 4715. (d) Tatay, S.; Gaviña, P.; Coronado, E.; Palomares., E. *Org. Lett.* **2006**, *8*, 3857. (e) Zhao, Y.; Zhong, Z. Q. *J. Am. Chem. Soc.* **2006**, *128*, 9988. (f) Nazeeruddin, M. K.; Di Censo, D.; Humphry-Baker, R.; Grätzel, M. *Adv. Funct. Mater.* **2006**, *16*, 189. (g) Coronado, E.; Galán-Mascarós, J. R.; Martí-Gastaldo, E.; Palomares, C.; Durrant, J. R.; Vilar, R.; Grätzel, M.; Nazeeruddin, M. K. *J. Am. Chem. Soc.* **2005**, *127*, 12351. (h) Balaji, T.; El-Safty, S. A.; Matsunaga, H.; Hanaoka, T.; Mizukami, F. *Angew. Chem., Int. Ed.* **2006**, *45*, 7202. (i) Lin, S. Y.; Wu, S. M.; Chen, C. H. *Angew. Chem., Int. Ed.* **2006**, *45*, 4948.
(15) (a) Jiménez, D.; Martínez-Máñez, R.; Sancenón, F.; Soto, J. *Tetrahedron Lett.* **2004**, *45*, 1257. (b) Caballero, A.; Lloveras, V.; Curiel, D.; Tárraga, A.; Espinosa, A.; García, R.; Vidal-Gancedo, J.; Rovira, C.; Wurst, K.; Molina, P.; Veciana, J. *Inorg. Chem.* **2007**, *46*, 825.
(16) (a) Hennrich, G.; Sonnenschein, H.; Resch-Genger, U. *J. Am. Chem. Soc.* **1999**, *121*, 5073. (b) Nolan, E. M.; Lippard, S. J. *J. Am. Chem. Soc.* **2003**, *125*, 14270. (c) Ros-Lis, J. V.; Marcos, M. D.; Martínez-Máñez, R.; Rurack, K.; Soto, J. *Angew. Chem., Int. Ed.* **2005**, *44*, 4405. (d) Kimand, I. B.; Bunz, U. H. F. *J. Am. Chem. Soc.* **2006**, *128*, 2818. (e) Kim, I. B.; Erdogan, B.; Wilsonand, J. N.; Bunz, U. H. F. *Chem.—Eur. J.* **2004**, *10*, 6247. (f) Ou, S. J.; Lin, Z. H.; Duan, C. Y.; Zhang, H. T.; Bai, Z. P. *Chem. Commun.* **2006**, 4392.
(17) McClure, D. S. *J. Chem. Phys.* **1952**, *20*, 682.
(18) Métivier, R.; Leray, I.; Valeur, B. *Chem.—Eur. J.* **2004**, *10*, 4480.
(19) Moon, S. Y.; Youn, N. J.; Park, S. M.; Chang, S. K. *J. Org. Chem.* **2005**, *70*, 2394.
(20) Zhu, X. J.; Fu, S. T.; Wong, W. K.; Guo, J. P.; Wong, W. Y. *Angew. Chem.* **2006**, *45*, 3222.
(21) Kim, S. H.; Song, K. C.; Ahn, S.; Kang, Y. S.; Chang, S. K. *Tetrahedron Lett.* **2006**, *47*, 497.
(22) Yu, Y.; Lin, L. R.; Yang, K. B.; Zhong, X.; Huang, R. B.; Zheng, L. S. *Talanta* **2006**, *69*, 103.
(23) Pandey, S.; Azam, A.; Chawla, H. M. *Org. Biomol. Chem.* **2009**, *7*, 269.
(24) Elanchezhian, V. S.; Kandaswamy, M. *Inorg. Chem. Commun.* **2010**, *13*, 1109.
(25) Nolan, E. M.; Lippard, S. J. *J. Am. Chem. Soc.* **2003**, *125*, 14270.
(26) Nolan, E. M.; Lippard, S. J. *J. Am. Chem. Soc.* **2007**, *129*, 5910.
(27) Avirah, R. R.; Jyothish, K.; Ramaiah, D. *Org. Lett.* **2007**, *9*, 121.
(28) He, G. J.; Zhao, Y. G.; He, C.; Liu, Y.; Duan, C. Y. *Inorg. Chem.* **2008**, *47*, 5169.
(29) Hirata, S.; Sakai, T.; Kitamura, N.; Kubukawa, K.; Kutsumura, N.; Otani, T.; Saito, T. *Tetrahedron* **2010**, *66*, 653.
(30) Thakur, A.; Adarsh, N. N.; Chakraborty, A.; Devi, M.; Ghosh, S. *J. Organomet. Chem.* **2010**, *695*, 1059.
(31) (a) López, J. L.; Tárraga, A.; Espinosa, A.; Velasco, M. D.; Molina, P.; Lloveras, V.; Vidal-Gancedo, J.; Rovira, C.; Veciana, J.; Evans, D. J.; Wurst, K. *Chem.—Eur. J.* **2004**, *10*, 1815. (b) Martinez, R.; Espinosa, A.; Tárraga, A.; Molina, P. *Org. Lett.* **2005**, *7*, 5869. (c) Zapata, F.; Caballero, A.; Espinosa, A.; Tárraga, A.; Molina, P. *Org. Lett.* **2007**, *9*, 2385.

(32) Lloveras, V.; Caballero, A.; Tárraga, A.; Velasco, M. D.; Espinosa, A.; Wurst, K.; Evans, D. J.; Vidal-Gancedo, J.; Rovira, C.; Molina, P.; Veciana, J. *Eur. J. Inorg. Chem.* **2005**, 2436.

(33) (a) Chesney, A.; Bryce, M. R.; Batsanov, A. S.; Howard, J. A. K.; Goldenberg, L. M. *Chem. Commun.* **1998**, 677. (b) Beer, P. D.; Smith, D. K. *J. Chem. Soc., Dalton Trans.* **1998**, 417. (c) Carr, J. D.; Coles, S. J.; Hassan, W. W.; Hursthouse, M. B.; Malik, K. M. A.; Tucker, J. H. R. *J. Chem. Soc., Dalton Trans.* **1999**, 57.

(34) Lakowicz, J. R. *Principles of Fluorescence Spectroscopy*, 3rd ed.; Springer: New York, 2006.

(35) Geddes, C. D.; Lakowicz, J. R. *Advanced Concepts in Fluorescence Sensing: Small Molecule Sensing Topics in Fluorescence Spectroscopy*; Springer: New York, 2005; Vol. 9.

(36) The fluorescence quantum yields were measured with respect to fluoresein as the standard ($\Phi = 0.79$; Dawson, W. R.; Windsor, M. W. *J. Phys. Chem.* **1968**, *72*, 3251–3260) using the equation $\Phi_x/\Phi_s = (S_x/S_s)[(1 - 10^{-A_s})/(1 - 10^{-A_x})]^2(n_s^2/n_x^2)$, where x and s indicate the unknown and standard solutions, respectively, Φ is the quantum yield, S is the area under the emission curve, A is the absorbance at the excitation wavelength ($\lambda = 434$ nm), and n is the index of refraction..

(37) CHEF is defined as I_{max}/I_0, where I_{max} corresponds to the maximum emission intensity of the receptor−metal complex and I_0 is the maximum emission intensity of the free receptor.

(38) (a) Mallick, A.; Chattopadhyay, N. *Photochem. Photobiol.* **2005**, *81*, 419. (b) Benesi, H. A.; Hildebrand, J. H. *J. Am. Chem. Soc.* **1949**, *71*, 2703.

(39) The binding constant value of Hg^{2+} with **3** has also been determined from the emission intensity data and is similar to that of the value of **2** ($K = 4.11 \times 10^6$ M^{-1}; Supporting Information, Figure S13).